AD-A113 074 MISSOURI UNIV-COLUMBIA F/G 6/18
A COMPREHENSIVE MATHEMATICAL MODEL OF THE CARDIOVASCULAR SYSTEM--ETC(U)
OCT 81 X J AVULA AFOSR-80-0128
UNCLASSIFIED AFOSR-TR-82-0211 NL

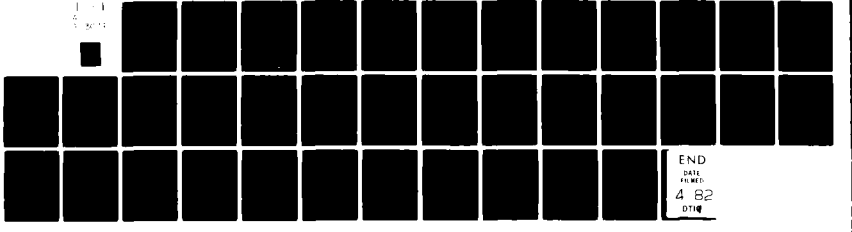

END
DATE FILMED
4 82
DTIC

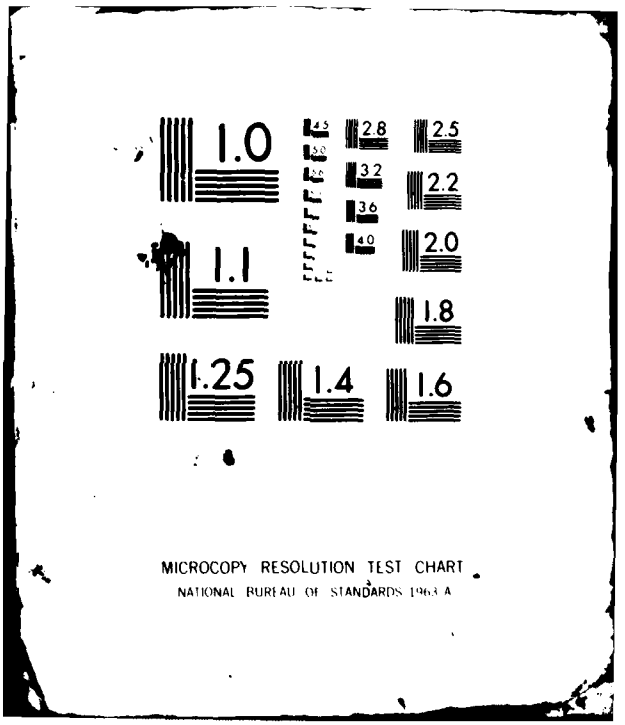
1.0
1.1
1.25
1.4
1.6
2.8
3.2
3.6
4.0
2.5
2.2
2.0
1.8
MICROCOPY RESOLUTION TEST CHART
NATIONAL BUREAU OF STANDARDS 1963 A

UNCLASSIFIED

SECURITY CLASSIFICATION OF THIS PAGE (When Data Entered)

REPORT DOCUMENTATION PAGE	READ INSTRUCTIONS BEFORE COMPLETING FORM
1. REPORT NUMBER AFOSR-TR- 82-0211	2. GOVT ACCESSION NO. AD-A113074 / 3. RECIPIENT'S CATALOG NUMBER
4. TITLE (and Subtitle) A Comprehensive Mathematical Model of the Cardiovascular System Under Time-Dependent Acceleration Stress	5. TYPE OF REPORT & PERIOD COVERED Final Technical
	6. PERFORMING ORG. REPORT NUMBER
7. AUTHOR(s) Xavier J. R. Avula	8. CONTRACT OR GRANT NUMBER(s) AFOSR-80-0128
9. PERFORMING ORGANIZATION NAME AND ADDRESS University of Missouri-Rolla c/o The Curators of the University of Missouri 215 University Hall, Columbia, MO 65201	10. PROGRAM ELEMENT, PROJECT, TASK AREA & WORK UNIT NUMBERS 2312/A1 (61102F)
11. CONTROLLING OFFICE NAME AND ADDRESS Life Sciences Directorate/NL Air Force Office of Scientific Research/NL Bolling Air Force Base, DC 20332	12. REPORT DATE 31 October 1981
	13. NUMBER OF PAGES 34
14. MONITORING AGENCY NAME & ADDRESS (if different from Controlling Office)	15. SECURITY CLASS. (of this report) Unclassified
	15a. DECLASSIFICATION/DOWNGRADING SCHEDULE

16. DISTRIBUTION STATEMENT (of this Report)

Approved for public release; distribution unlimited.

17. DISTRIBUTION STATEMENT (of the abstract entered in Block 20, if different from Report)

DTIC ELECTE MAR 0 6 1982 E

18. SUPPLEMENTARY NOTES

19. KEY WORDS (Continue on reverse side if necessary and identify by block number)

Mathematical Modeling, Cardiovascular System, Time-dependence, Acceleration.

20. ABSTRACT (Continue on reverse side if necessary and identify by block number)

In this study a comprehensive mathematical model of the cardiovascular system under time-dependent accelerations is developed. Recently developed high performance aircraft would expose the human body to acceleration injury if appropriate life-supporting devices are not incorporated in the design. To aid in the construction of desirable life support systems for aerospace maneuvers, the deformation of the arterial and venous segments under dynamic fluid loads caused by blood pooling duzing G_z acceleration are calculated. (cont.)

DD FORM 1 JAN 73 1473 EDITION OF 1 NOV 65 IS OBSOLETE

UNCLASSIFIED

SECURITY CLASSIFICATION OF THIS PAGE (When Data Entered)

20. ABSTRACT (cont.)

Linearized Navier-Stokes equations for blood flow and equations of large elastic deformation theory for blood vessel deformations are used. The resulting nonlinear partial differential equations are solved numerically. The model presented here consists of a closed-loop hydrodynamic system including the heart pump, compartments of large arteries and veins in the upper and lower body, and a baroreceptor feed back mechanism. To verify the model aortic pressure is calculated for an experimental deceleration profile. A satisfactory agreement between the theory and experiment is found.

AFOSR Grant Number: AFOSR 80-0128
Final Technical Report
31 October 1981

A comprehensive Mathematical Model of of the Cardiovascular System Under Time-Dependent Acceleration Stress

Dr. Avula

University of Missouri-Rolla
Rolla, MO 65401

Controlling Office: USAF Office of Scientific Research/NL
Bolling Air Force Base, DC 20332

A COMPREHENSIVE MATHEMATICAL MODEL OF THE CARDIOVASCULAR SYSTEM UNDER TIME-DEPENDENT ACCELERATION STRESS

Xavier J. R. Avula
Department of Engineering Mechanics
University of Missouri-Rolla
Rolla, Missouri 65401

ABSTRACT

In this study a comprehensive mathematical model of the cardiovascular system under time-dependent accelerations is developed. Recently developed high performance aircraft would expose the human body to acceleration injury if appropriate life-supporting devices are not incorporated in the design. To aid in the construction of desirable life support systems for aerospace maneuvers, the deformation of the arterial and venous segments under dynamic fluid loads caused by blood pooling during G_z acceleration are calculated. Linearized Navier-Stokes equations for blood flow and equations of large elastic deformation theory for blood vessel deformations are used. The resulting nonlinear partial differential equations are solved numerically. The model presented here consists of a closed-loop hydrodynamic system including the heart pump, compartments of large arteries and veins in the upper and lower body, and a baroreceptor feed back mechanism. To verify the model aortic pressure is calculated for an experimental deceleration profile. A satisfactory agreement between the theory and experiment is found.

NOMENCLATURE

A = Material constant in the strain energy function
B = Material constant in the strain energy function
B = (with sub- and superscripts) = Surface metric tensor

F = Body force

f = Acceleration

G = Determinant of the covariant metric tensor G_{ij}

g = Determinant of the covariant metric tensor g_{ij}

G_{ij} = Covariant metric tensor for reference coordinates of the deformed state

G^{ij} = Contravarient metric tensor for reference coordinates of the deformed state

g_{ij} = Covariant metric tensor for reference coordinates of the undeformed state

g^{ij} = Contravariant metric tensor for reference coordinates of the undeformed state

$2h_o$ = Wall thickness of the blood vessel

I_1, I_2, I_3 = Strain invariants

L = Length of blood vessel element

$n^{\alpha\beta}$ = Stress resultant tensor

p = pressure

Q = Flow rate

R_1 = Internal radius of the blood vessel

r = Radial coordinate

t = time

u, w = Radial and axial fluid velocity components

W = Strain energy function

z = Axial coordinate

$\Gamma^{\alpha}_{\beta\rho}$ = Christoffel symbol of the second kind

$\dot{\gamma}$ = Shear rate in blood

λ = Stretch ratio

μ = Coefficient of viscosity of blood

ν = Kinematic viscosity of blood

ρ = Mass density of blood vessel

ρ_o = Mass density of blood

τ^{ij} = Stress tensor

ϕ = A function of strain energy

Ψ = A function of strain energy

Subscripts and Superscripts

$i, j, k = 1, 2, 3$

$r, s = 1, 2$

$\alpha, \beta = 1, 2$

INTRODUCTION

The human body is well accustomed to the earth's force of gravity, but recent space age developments have occasioned its exposure to the hazards of high and abnormal gravitational fields, which are manifested in the form of vibration, impact, weightlessness, and positive, negative, forward, backward, and angular accelerations that are beyond its tolerance levels. Abnormal accelerations on the human body are known to cause headache, abdominal pain, impairment of vision, hemorrhage, and fracture depending upon the severity and kind[1-3]. The cardiovascular system in being central to the homeostasis of the organism is extremely susceptible to hostile changes in environmental force. The design of protective devices, which are expected to provide acceleration tolerance for the organism during aircraft and spacecraft maneuvers, must take into consideration the response of the cardiovascular system to acceleration stress. Therefore, a thorough understanding of the system and its structure-function relationship in an abnormal force environment is essential to any effort directed to overcome the acceleration trauma.

The prohibitiveness of actually subjecting the human body to abnormal accelerations to gain knowledge of the cardiovascular system's response is obvious. The alternative is to develop a mathematical model and to investigate the response of the system. The need for mathematical models and the analysis of model features for prediction of system performance are well recognized in view of the cost and risk involved in testing the original system. Theoretical analyses are extremely helpful for evaluating the relative

injury potential for various acceleration functions, in guiding experimental investigations, and in developing and understanding protective measures. Mathematical procedures also provide the basis for establishing precise dynamic and physiological scaling laws needed to translate experimental data obtained with various species into meaningful results for humans.

There is no dearth of mathematical models of the cardiovascular system in the scientific literature. Womersley[4] and Noordergraaf[5] presented a mathematical analysis of some aspects of the cardiovascular system by using a lumped parameter model. Taylor,[6] Kenner,[7] and Attinger et al.[8] used distributive parameter models to analyze pressure - flow relationships in arteries and veins. It is generally believed that a lumped parameter model is superior to the distributive one in the evaluation of overall cardiovascular system performance. Beneken and DeWit[9] characterized a large analog model of the entire human circulatory system in the form of approximately 40 equations. Rigorous mathematical formulations and extensive physiological information, including the factors affecting contractility of the myocardium, the effect of intrathoracic and abdominal pressure changes on the venous conductance and the ventricular distention, the baroreceptor reflex control of the cardiac pump and vascular resistance, the autoregulation in various vascular beds, and capillary fluid shift and stress relaxation phenomena were introduced into the model. It has been demonstrated that the model provides quick solutions for parametric sensitivity tests. Guyton and Coleman[10] presented an analog model of long-term circulatory regulation and emphasized the integration of the long-term autoregulation of the systemic vascular system into the basic scheme as the most powerful control mechanism for tissue homeostasis. Pennock and Attinger[11] proposed a mathematical model to analyze the

overall performance of the oxygen transport system. This model was represented by six equations and used to describe oxygen transfer and transport and normal performance. The changes on the interaction of subsystems and on optimization with respect to flexibility and maximal limits of performance were examined by altering various parameters. McLeod[12] proposed a physiological simulation benchmark experiment (PHYSBE) to economize on programming efforts and to establish bases for a comparison of various types of computer models of circulation. Sagawa[13,14] described the overall circulatory regulation and the mechanical properties of the cardiovascular system in the control of circulation. Camill[15] studied the response of the human cardiovascular system to whole-body sinusoidal vibrations by using an open-loop analog model of the standing and sitting man. Boyers et al.[16] simulated the steady state response of the human cardiovascular system with normal responses to change the posture, blood loss, transfusion, and autonomic blockage. Collins et al.[17] presented a dynamic, mathematical simulation of the cardiopulmonary system. Several articles related to blood flow in arteries have appeared in the book by McDonald[18]. An elastic tube theory of blood flow has been treated by Lambert[19] and Skalak and Stathis[20]. Kivity and Collins[21] presented a viscoelastic tube model for aortic rupture under decelerative forces. Rudinger[22] studied the effect of shock waves on mathematical models of aorta for better understanding of the behavior of the actual aorta.

Most of the above modeling efforts deal with electrical analogs of the cardiovascular system in which various parameters are introduced in terms of resistances, impedances, and capacitances. Because the measured or postulated values of these parameters are variable and their representation under high-g conditions is speculative, errors of large magnitude are likely to creep into the model. Therefore, an analysis that is based purely on the original properties of the cardiovascular elements coupling

the fluid-flow, deformation of the vascular walls, and the material properties of the blood vessels and surrounding tissue is expected to yield a better mathematical model.

To understand the blood flow characteristics in the arterial system, the knowledge of the material properties of the arterial wall is essential. Bergel[23], Fung[24], Demiray and Vito[25] have utilized mathematical models of the constitutive properties of the arterial tissue to determine the stresses in the arterial walls. In the present study, the strain energy function given by Demiray and Vito[25] for an arterial wall specimen has been used in determining the aortic pressure that is compatible with large deformation of the aorta and the associated flow under acceleration stress.

The present study also considers the effect of acceleration on the mircrocirculation. Microcirculation under normal conditions was investigated by Prothero and Burton[26], Whitmore[27], Gross and Aroesty[28], Gross and Intaglietta[29], Skalak[30] and Fung[31] who presented various theories of flow in the capillary bed connecting the arteries and veins.

Several experimental investigations on the effects of acceleration stress on the human body have been performed at the USAF School of Aerospace Medicine at Brooks Air Force Base, Texas. Burton[32] subjected miniature swine to G_z acceleration to study its effects on the organism and extrapolated the results to human beings. Parkhurst, et al[33] conducted experiments on human tolerance to high $+G_z$ forces. Leverett, et al.[34] investigated the physiologic response to high sustained acceleration stress. Peterson, et al.[35] studied the cardiovascular responses during and following exposure to $+G_z$ forces in chronically instrumented anesthetized dogs. Burton and MacKenzie[36] determined the extent of heart pathology as a function of acceleration stress.

DESCRIPTION OF THE PHYSICAL MODEL

Because the cardiovascular system consists of several components, it would be too complicated to handle all of them in a general model. Although it would be desirable to include the behavior of each cardiovascular component under acceleration stress in the total modeling effort, certain components can be lumped together to simplify the analysis and still preserve the character of the system. In the proposed model, five elastic chambers containing blood are arranged in a closed loop, and a mathematical analysis is made to calculate the fluid shift under acceleration stress. The five elastic chambers are: 1) arteries of the thorax and the lower body, 2) veins of the thorax and the lower body, 3) arteries of the upper body, 4) veins of the upper body, and 5) heart and lungs. A schematic of the elastic reservoirs arranged in a closed loop is shown in Fig. 1. This physical system is then subjected to $\pm G_z$ acceleration. The elastic reservoirs are considered highly deformable, and the theory of large elastic deformations is applied to the calculation of their expansion under acceleration stress. The Navier-Stokes equations are used to determine the fluid velocity into and out of the chambers with proper boundary conditions to match the wall motion.

MATHEMATICAL MODELING

A. Equations of Fluid Motion

The geometry of the elastic tube containing blood in motion is shown in Fig. 2. Let r, θ, z be the cylindrical polar coordinates and let u, v, and w bet the velocity components in the corresponding directions. Assuming axial symmetry in flow and tube deformation, the linearized Navier-Stokes equations for the flow of blood can be written as:

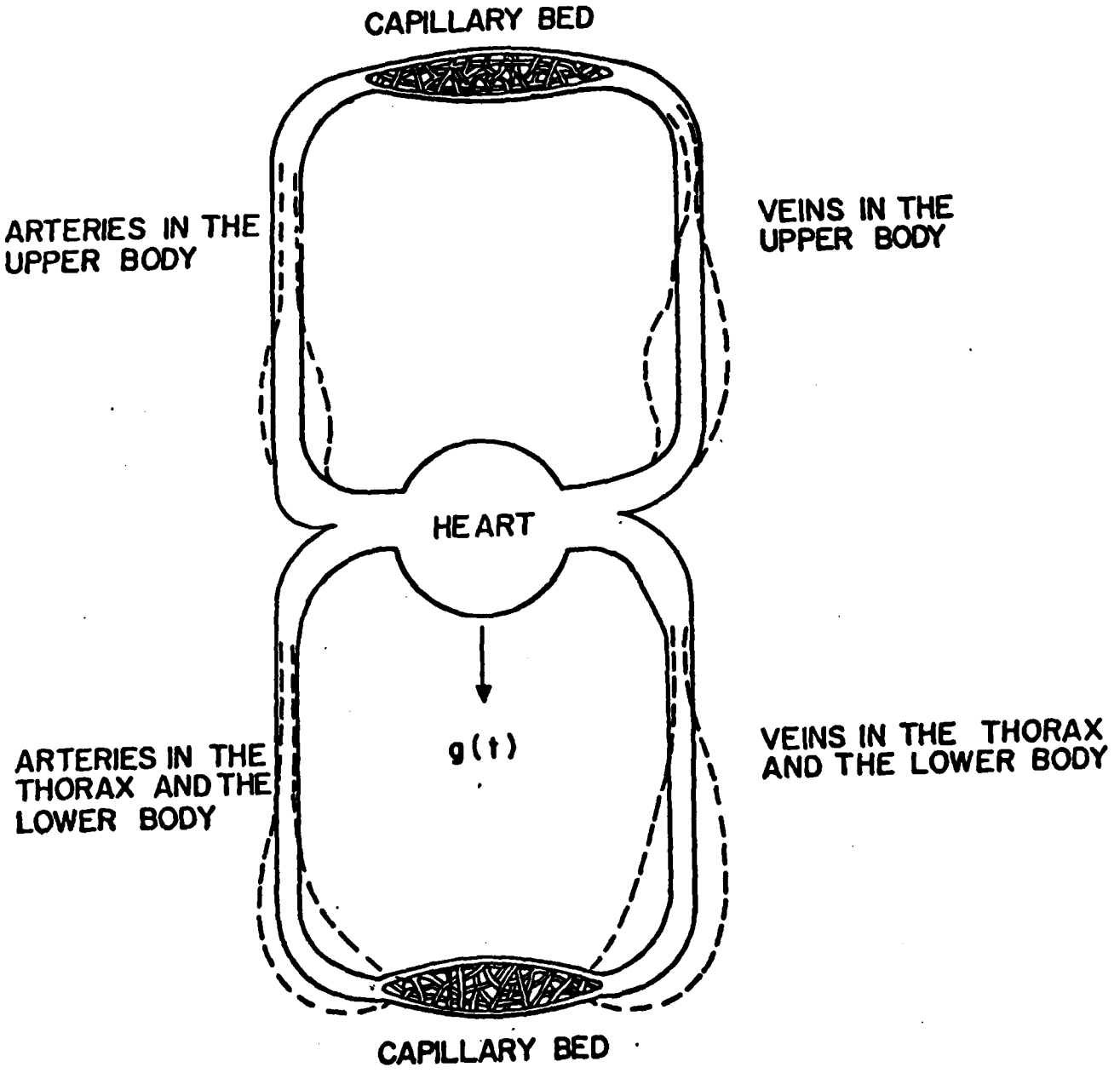

Fig. 1 Schematic of physical model

$$\frac{\partial u}{\partial t} = -\frac{1}{\rho_o}\frac{\partial p}{\partial r} + \nu\left(\frac{\partial^2 u}{\partial r^2} + \frac{1}{r}\frac{\partial u}{\partial r} + \frac{\partial^2 u}{\partial z^2} - \frac{u}{r^2}\right) \tag{1}$$

$$\frac{\partial w}{\partial t} = -\frac{1}{\rho_o}\frac{\partial p}{\partial z} + \nu\left(\frac{\partial^2 w}{\partial r^2} + \frac{1}{r}\frac{\partial w}{\partial r} + \frac{2w}{z^2}\right) + g(t) \tag{2}$$

where p is the pressure, ν is the kinematic viscosity, ρ_o is density of blood and g(t) is the body force per unit mass caused by the acceleration. The continuity equation is

$$\frac{\partial u}{\partial r} + \frac{u}{r} + \frac{\partial w}{\partial z} = 0 \tag{3}$$

The above equations are nondimensionalized using a typical length, R_o, which is the initial (undeformed) radius of the aorta, and U, the average velocity of blood in the aorta. Introducing the new quantities

$$t^* = \frac{tU}{R_o},\ r^* = \frac{r}{R_o},\ z^* = \frac{z}{R_o},\ w^* = \frac{w}{U}$$

$$u^* = \frac{u}{U},\ p^* = \frac{p}{\rho_o U^2},\ g^* = \frac{Rg}{U^2},\ Re = \frac{UR_o}{\nu} \tag{4}$$

the equations of motion and the continuity equation in terms of the newly defined variables become

$$\frac{\partial u^*}{\partial t^*} = -\frac{\partial p^*}{\partial r^*} + \frac{1}{Re}\left(\frac{\partial^2 u^*}{\partial r^{*2}} + \frac{1}{r^*}\frac{\partial u^*}{\partial r^*} + \frac{\partial^2 u^*}{\partial z^{*2}} - \frac{u^*}{r^{*2}}\right) \tag{5}$$

$$\frac{\partial w^*}{\partial t^*} = -\frac{\partial p^*}{\partial z^*} + \frac{1}{Re}\left(\frac{\partial w^{*2}}{\partial r^{*2}} + \frac{1}{r^*}\frac{\partial w^*}{\partial r^*} + \frac{\partial^2 w^*}{\partial z^{*2}}\right) + g^*(t^*) \tag{6}$$

$$\frac{\partial u^*}{\partial r^*} + \frac{u^*}{r^*} + \frac{\partial w^*}{\partial r^*} = 0 \tag{7}$$

Deleting the "stars" for simplicity, the governing equations in the dimensionless form will become

$$\frac{\partial u}{\partial t} = -\frac{\partial p}{\partial r} + \frac{1}{Re}\left(\frac{\partial^2 u}{\partial r^2} + \frac{1}{r}\frac{\partial u}{\partial r} + \frac{\partial u^2}{\partial z^2} - \frac{u}{r^2}\right) \tag{8}$$

$$\frac{\partial w}{\partial t} = -\frac{\partial p}{\partial z} + \frac{1}{Re}\left(\frac{\partial^2 w}{\partial r^2} + \frac{1}{r}\frac{\partial w}{\partial r} + \frac{\partial^2 w}{\partial z^2}\right) + g(t) \tag{9}$$

$$\frac{\partial u}{\partial r} + \frac{u}{r} + \frac{\partial w}{\partial z} = 0 \tag{10}$$

The boundary and initial conditions are

$$u = \frac{dR_1}{dt} \quad \text{at } r = R_1 \qquad t \geq 0$$

$$w = 0 \quad \text{at } r = R_1 \qquad t \geq 0 \tag{11}$$

$$w = 1 \quad \text{at } z = 0 \qquad t \geq 0$$

where R_1 is the inside radius of the blood vessel in the deformed state.

B. Equations of Motion for Thin-Walled Elastic Tube:

The theory of large elastic deformations is utilized to describe the time-dependent deformation of the blood vessels. In view of the published results on blood pooling and the consequent cardiac insufficiency, the application of large deformation theory appears necessary. Demiray and Vito[25] have previously used this theory to calculate the deformation of arteries.

The undeformed and deformed cylindrical tubes are shown in Fig. 3. Let r, θ, z represent a point in the wall of the undeformed tube, and R, θ, z in the deformed tube. r_1, r_2 are inside and outside radii, respectively, of the undeformed tube, and R_1, R_2 those of the deformed tube. Axial stretch of the tube is neglected because of tethering caused by the surrounding tissue. Assuming the material of the blood vessels to be homogeneous, incompressible, and isotropic, the stress at any point can be written as:

$$\tau^{ij} = \phi g^{ij} + \psi B^{ij} + PG^{ij} \tag{12}$$

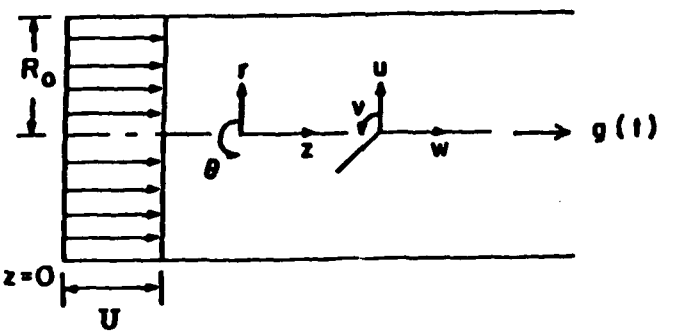

Fig. 2 Blood vessel geometry

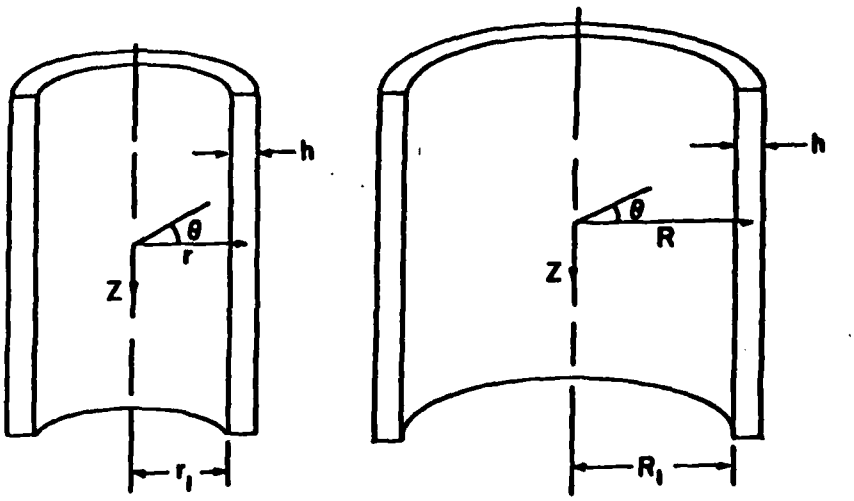

Fig. 3. Undeformed and deformed elastic tube

where $\phi = 2(\partial W/\partial I_1)$, $\psi = 2(\partial W/\partial I_2)$, $B^{ij} = I_1 g^{ij} - g^{ir}g^{js}G_{rs}$, P is a scalar function which represents a hydrostatic pressure, W is the strain energy function, I_1 and I_2 are the strain invariants, and g^{ij}, g_{ij}, G^{ij}, and G_{ij} are the contravariant and covariant metric tensors[37,38]. The indices i and j take the values 1, 2, and 3. The equations of motion are given by:

$$\tau^{ij}{}_{||\,i} + \rho_w F^j = \rho_w f^j \tag{13}$$

where $||$ denotes covariant differentiation, ρ_w is the density of the vessel wall, F is the body force, and f is the acceleration. Let us neglect the body force on the vessel wall in comparison to its effect on the fluid flowing in the cylindrical tube. Performing the covariant differentiation on the remaining part of the equation of motion we get

$$\tau^{ij}{}_{,i} + \Gamma^i{}_{ir}\,\tau^{rj} + \Gamma^i{}_{ir}\,\tau^{ir} = \rho_w f^j \tag{14}$$

where $\Gamma^i{}_{jk}$ represent the Christoffel symbols of the second kind[37,38].

It has been shown that for a biomaterial, a reasonable strain energy function as shown in Ref. 25 is

$$W = \frac{B}{2A}\left[e^{A(I_2 - 3)} - 1\right] \tag{15}$$

in which A and B are material constants. Defining the circumferential stretch ratio $\lambda = R/r$, the stresses in the r, θ, z directions can be expressed as

$$\tau^{11} = P + B\left(1 + \frac{1}{\lambda^2}\right) e^{A(I_2-3)} \tag{16}$$

$$R^2\tau^{22} = P + B(1 + \lambda^2)\, e^{A(I_2-3)} \tag{17}$$

$$\tau^{33} = P + B\left(\frac{1}{\lambda^2} + \lambda^2\right) e^{A(I_2-3)} \tag{18}$$

Substitution of the above equations and the appropriate Christoffel symbols in Eq. (14) gives the equation of motion in the form

$$\frac{\partial}{\partial R}\left[P + B\left(1 + \frac{1}{\lambda^2}\right) e^{A(I_2-3)}\right] + \frac{B}{R}\left(\frac{1}{\lambda^2} - \lambda^2\right) e^{A(I_2-3)} = \rho_w \frac{\partial^2 R}{\partial t^2} \tag{19}$$

The incompressibility condition leads to:

$$R^2 - R_1^2 = r^2 - r_1^2 \tag{20}$$

and

$$\frac{\partial^2 R}{\partial t^2} = -\frac{R_1^2}{R^3}\left(\frac{dR_1}{dt}\right)^2 + \frac{1}{R}\left(\frac{dR_1}{dt}\right)^2 + \frac{R_1}{R}\frac{d^2R_1}{dt^2} \tag{21}$$

With p_1, p_2 denoting the pressure on the inside and outside wall, respectively, of the blood vessel, the use of the boundary conditions, $\tau^{11} = -p_1(t)$ at $R = R_1$ and $\tau^{11} = -p_2(t)$ at $R = R_2$, substituting Eq. (21) into Eq. (19) and integrating yields

$$p_1(t) - p_2(t) = \rho w R_1 \frac{d^2R_1}{dt^2} \ln\frac{R_2}{R_1} + \left(\frac{dR_1}{dt}\right)^2 \rho_w \left[\ln\frac{R_2}{R_1} + \frac{1}{2}\left(\frac{R_2^2}{R_1^2} - 1\right)\right]$$

$$- B\int_{\lambda_1}^{\lambda_2} \frac{1+\lambda^2}{\lambda^3} e^{A\left(\lambda^2 + \frac{1}{\lambda^2} - 2\right)} d\lambda \tag{22}$$

It must be recognized that the relationship $I_2 = 1 + \lambda^2 + 1/\lambda^2$ has been used to obtain Eq. (22).

The following dimensionless quantities are introduced into Eq. (22):

$$p^* = \frac{P}{\rho_o U^2}, \quad R_1^* = \frac{R_1}{R_o}, \quad R_2^* = \frac{R_2}{R_o}, \quad t^* = \frac{tU}{R_o}, \quad B^* = \frac{B}{\rho_o U^2}, \quad \rho_w^* = \frac{\rho_w}{\rho_o} \tag{23}$$

Then the equation of motion in the radial direction becomes

$$(p_1^* - p_2^*) = \rho_w^* \, R_1^* \frac{d^2R_1^*}{dt^{*2}} \ln \left(\frac{R_2^*}{R_1^*}\right) + \rho_w^* \left(\frac{dR^*}{dt^*}\right)^2 \left[\ln \frac{R_2^*}{R_1^*} + \frac{1}{2} \frac{R_2^{*2}}{R_1^{*2}} - 1\right)] - B^* \int_{\lambda_1}^{\lambda_2} \frac{1+\lambda^2}{\lambda^3} e^{A(\lambda^2 + 1/\lambda^2 - 2)} d\lambda \tag{24}$$

If the "stars" are dropped for convenience, Eq. (24) can be written as:

$$p_1(t) - p_2(t) = \rho_w R_1 \frac{d^2R_1}{dt^2} \ln \frac{R_2}{R_1} - \rho_w \left(\frac{dR_1}{dt}\right)^2 \left[\ln \frac{R_2}{R_1} + \frac{1}{2}\left(\frac{R_2^2}{R_1^2} - 1\right)\right] - B \int_{\lambda_1}^{\lambda_2} \frac{1+\lambda^2}{\lambda 3} e^{A(\lambda^2 + 1/\lambda^2 - 2)} d\lambda \tag{25}$$

The initial conditions are:

At time $t = t_o$, $R_1 = R_o$, $dR_1/dt = u$, radial velocity of fluid.

In the above derivation, it must be noted that only the radial displacements of the blood vessels are considered significant since the axial displacements are prevented by tethering of the vessels to the surrounding tissue.

C. Equations of Left Ventricular Contraction

In view of the large volume changes of the left ventricle between the systole and the diastole, the theory of large elastic deformation is used to analyze the pumping action of the heart. In first approximation, the components of the pulmonary circulation and the left ventricle are lumped together and the system is treated as a highly deformable sphere undergoing radial deformation of the left ventricle by using a strain energy function of the type represented in Eq. (15).

The undeformed and deformed configurations of a spherical chamber are shown in Fig. 4. Let a point located by r, θ, ϕ in the undeformed sphere be displaced to a new location R, θ, ϕ in the deformed sphere. Eqs. (12-15) in the previous section, being general, are valid for the deformation of the sphere also. However, the stresses are expressed in the form

$$\tau^{11} = p + B\, e^{A(I_2 - 3)}$$

$$\tau^{22} = \frac{p}{R^2} + \frac{Be}{R^2}^{A(I_2 - 3)}(1/\lambda^2 + \lambda^4) \tag{26}$$

$$\tau^{33} = \frac{\tau^{22}}{\sin^2\theta}$$

where $\lambda = R/r$ and $I_2 = \lambda^4 + 2/\lambda^2$. The equation of motion in the radial direction is

$$\frac{\partial}{\partial R}\left(p + \frac{2B}{\lambda^2}\, e^{A(I_2-3)}\right) + \frac{2B}{R}\, e^{A(I_2-3)}\left(\frac{1}{\lambda^2} - \lambda^4\right) = \frac{\partial^2 R}{\rho \partial t^2} \tag{27}$$

The incompressibility condition leads to

$$\frac{\partial^2 R}{\partial t^2} = \frac{2R_1^4}{R^5}\left(\frac{dR_1}{dt}\right)^2 + \frac{2R_1}{R^2}\left(\frac{dR_1}{dt}\right)^2 + \frac{R_1^2}{R^2}\,\frac{d^2R_1}{dt^2} \tag{28}$$

Substituting Eq. (28) into (27) and noting the boundary conditions

$$\tau^{11} = -p_1(t)$$
$$\tau^{22} = -p_2(t) \tag{29}$$

and integrating with respect to R, the equation of motion can be put in the form:

$$p_1(t) - p_2(t)$$

$$= -\int_{\lambda_1}^{\lambda_2} \frac{2B}{\lambda^3} e^{A(\lambda^4 + 2/\lambda^2 - 3)} (\lambda^3 + 1)\, d\lambda$$

$$+ \rho R_1^2 \frac{d^2R_1}{dt^2} \left(\frac{1}{R_1} - \frac{1}{R_2}\right) + 2\rho R_1 \left(\frac{dR_1}{dt}\right)^2 \left(\frac{1}{R_1} - \frac{1}{R_2}\right)$$

$$- \frac{\rho R_1^4}{2} \left(\frac{dR_1}{dt}\right)^2 \left(\frac{1}{R_1^4} - \frac{1}{R_2^4}\right) \qquad (30)$$

Using the dimensionless variables described in Eq. (23) the nondimensional form of the equation of motion becomes:

$$p_1^* - p_2^* =$$

$$-2_B^* \int_{\lambda_1}^{\lambda_2} \left(1 + \frac{1}{\lambda^3}\right) e^{A(\lambda^4 + 2/\lambda^2 - 3)}\, d\lambda$$

$$+ (R_1^*)^2 \rho^* \frac{d^2R_1}{dt^{*2}} \left(\frac{1}{R_1^*} - \frac{1}{R_2^*}\right) \lambda$$

$$+ 2R_1^* \rho^* \frac{dR_1^*}{dt^*} \left(\frac{1}{R_1^*} - \frac{1}{R_2^*}\right)$$

$$- \frac{\rho^* R_1^{*4}}{2} \left(\frac{dR_1^*}{dt^*}\right)^2 \left(\frac{1}{R_1^{*4}} - \frac{1}{R_2^{*4}}\right) \qquad (31)$$

Deleting the "stars" for convenience, the equation of motion can now be put in the form:

$$p_1(t) - p_2(t) =$$

$$-2_B \int_{\lambda_1}^{\lambda_2} \left(1 + \frac{1}{\lambda 3}\right) e^{A(\lambda^4 + 2/\lambda^2 - 3)} d\lambda$$

$$+ \rho R_1^2 \frac{d^2R_1}{dt^2} \left(\frac{1}{R_1} - \frac{1}{R_2}\right)$$

$$+ 2\rho R_1 \left(\frac{dR_1}{dt}\right)^2 \left(\frac{1}{R_1} - \frac{1}{R_2}\right)$$

$$- \rho \frac{R_1^4}{2} \left(\frac{dR_1}{dt}\right)^2 \left(\frac{1}{R_1^4} - \frac{1}{R_2^4}\right) \qquad (32)$$

The initial conditions are:

At time $t = t_o$, $R_1 = R_o$, $dR_1/dt = u_R$, a time function which depends upon the venous return. It must be noted that the transmural pressure across the myocardium in Eq. (32) is not the same as the pressure difference in Eq. (25).

For a complete solution Eqs. 8, 9, 10, 25 and 32 must be simultaneously solved with the appropriate initial and boundary conditions in conjunction with a reasonable baroreceptor control mechanism.

D. Baroreceptor Reflex Control

The baroreceptor control of the systemic arterial pressure is accomplished by a closed loop regulator which continuously monitors the systemic pressure through baroreceptors located in the carotid sinus and in the aortic arch[39]. A typical steady-state relationship between the input pressure (feedback) and the output pressure (regulated systemic arterial pressure), as described by Taylor[40], is shown in Fig. 5. Since it has been observed in several cardiovascular system experiments under acceleration stress that the response of the baroreceptor reflex mechanism begins in G-8 seconds after the pressure change, it is reasonable to use the steady-state curve of Fig. 5 for model response under high sustained acceleration. For short duration, impact type accelerations this curve would be unsuitable.

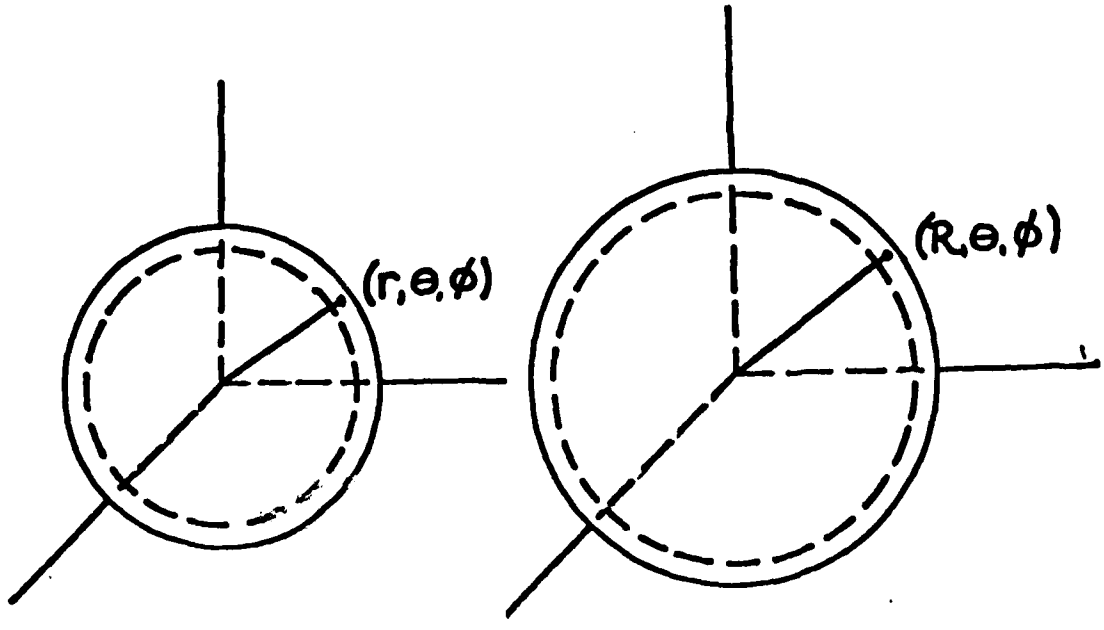

Fig. 4. Undeformed and deformed representation of the left ventricle

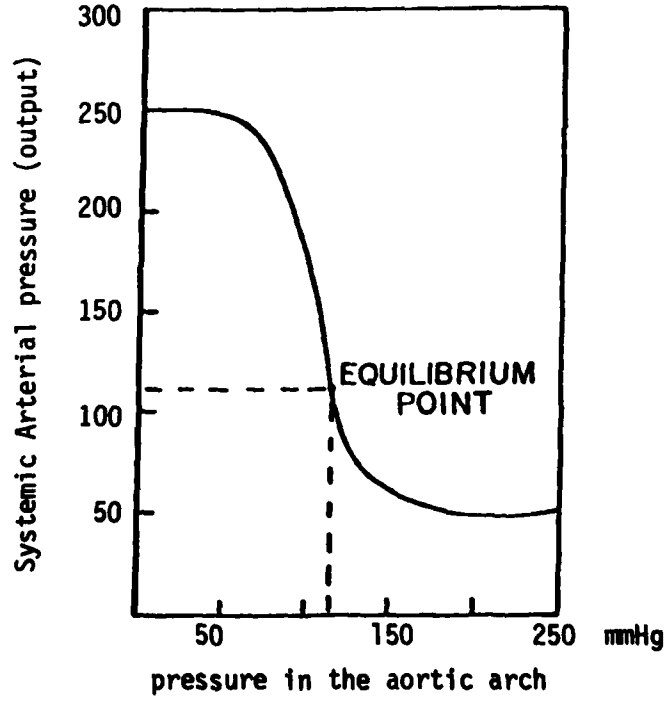

Fig. 5 Input-output pressure relationship in baroreceptor control

E. Effect of Acceleration on Microcirculation

The blood vessels of microcirculation are extraordinarily small, and their typical dimensions are of the order of microns. Under normal circumstances, the velocity of the blood in the microcirculation is 1 mm/sec and the Reynolds number is of the order $O(10^{-3})$, which is sufficiently small so that the Stokes flow approximations are applicable. Neglecting the inertial effects and assuming that the stream lines are nearly parallel, the dimensionless equation of fluid motion in the axial (z) direction becomes

$$\frac{\partial w}{\partial t} = - \frac{\partial p}{\partial z} + \frac{1}{Re} \left(\frac{\partial^2 w}{\partial r^2} + \frac{1}{r} \frac{\partial w}{\partial r} + \frac{\partial^2 w}{\partial z^2}\right) + g(t) \qquad (33)$$

which can be rearranged to read

$$Re \frac{\partial w}{\partial t} = - Re \left(\frac{\partial p}{\partial z}\right) + \left(\frac{\partial^2 w}{\partial r^2} + \frac{1}{r} \frac{\partial w}{\partial r} + \frac{\partial^2 w}{\partial z^2}\right) + Re\ g(t) \qquad (34)$$

In the earth's natural gravitational field, the dimensionless g, as given in Eq. (4), is of the order $O(10^{-2})$, and with the effect of Re $O(10^{-3})$ in the last term Re g(t) in Eq. (34) becomes physiologically insignificant, being of the order $O(10^{-5})$. We estimate that the effect of acceleration on microcirculation per se can be safely neglected up to 100 g. However, the pressure of the blood pooled in the arteries and veins can affect the flow rate in the small vessels. For this reason it is necessary to determine a relationship between the pressure gradient and the flow rate in the small blood vessels.

For the flow of a Newtonian fluid in a uniform tube Szymanski[41] showed that the flow would be fully developed if $\nu t/D^2 > 1$, where t = time, ν = kinematic viscosity, and D = tube diameter. An extension of this criterion to microcirculation yields $\nu\Delta/D^2 > 1$ for flow to be quasi-steady, where Δt is the smallest characteristic time of the unsteadiness in flow.

According to Burton[42], $\Delta t \simeq 0.1$ sec; using $\nu = 0.04$ Stokes, one finds that the diameter D must be greater than 600μ (microns) for any significant effect of unsteadiness. Since, in microcirculation the diameters of blood vessels are much less than 600μ, changes in flow due to unsteadiness become entirely negligible. On this basis Benis[43] argued that the effect of unsteadiness on non-Newtonian flow could also be neglected. Thus, the use of steady-flow equations can be justified for microcirculation.

For steady capillary flow, the flow rate through a circular tube can be expressed by

$$Q = 2\pi \int_0^R rw \, dr \tag{35}$$

where Q = flowrate, R = tube radius, and w = blood velocity. Integration by parts of the right hand side yields

$$Q = \pi \int_0^R d(r^2 w) - \pi \int_0^R r^2 \left(\frac{dw}{dr}\right) dr \tag{36}$$

The first integral on the right hand side of Eq. (36) is zero. In the second integral the domain of integration can be divided into two regions: a cone of unsheared fluid extending to radius R_y, and the annular region bounded by the unsheared fluid and the tube wall. Then,

$$Q = -\pi \int_0^{R_y} r^2 \left(\frac{dw}{dr}\right) dr - \pi \int_{R_y}^R r^2 \left(\frac{dw}{dr}\right) dr \tag{37}$$

The first term on the right hand side in Eq. (37) which represents the core integral is zero. By changing the variables from r to τ in the second term as suggested by Merrill et. al.[44], Eq. (37) can be written as

$$Q = \frac{8\pi}{(\Delta P/L)^3} \int_{\tau_y}^{\tau_w} \tau^2 \dot{\gamma} \, d\tau \tag{38}$$

where L = length of the capillary

ΔP = pressure drop

τ = shear stress

$\dot{\gamma}$ = shear rate.

The shear stress and the shear rate are related by an empirical equation

$$\tau^{1/2} = \tau_y^{1/2} + \mu^{1/2}\,\dot{\gamma}^{1/2} \tag{39}$$

in which τ_y is the yield shear stress, and $\mu^{1/2}$ is a constant which represents the slope of the Casson plot relating the viscometric parameters of blood. In Poiseuille's flow μ becomes the blood viscosity. Substitution of Eq. (39) into Eq. (38) and integration yields

$$Q = \frac{\pi R^4(\Delta P/L)}{8\mu} - \frac{4\pi\,\tau_y^{1/2}\,R^{7/2}\,(\Delta P/L)^{1/2}}{7\sqrt{2}\,\mu} - \frac{2\pi\,\tau_y^{4}}{21(\Delta P/L)^3\mu} + \frac{\pi\,\tau_y\,R^3}{3\mu} \tag{40}$$

which is valid under the assumption that the flow is steady, laminar and incompressible, and blood is homogeneous. In the above equation, τ_y and μ are known constants; then plots of Q vs. $\Delta P/L$ for capillaries of various radii can be easily constructed. An example of this relationship is shown in Fig. 6.

RESULTS AND DISCUSSION

The system of equations (8), (9), (10), (15), (25) and (32) constitute the basic hydrodynamic model in this study. These equations are nonlinear and coupled and therefore a closed-form solution cannot be found. They were solved numerically on a digital computer by a finite difference scheme. The numerical data for arterial segments were taken from Westerhof[45] and are presented here in Table I. Although the arterial segments were presented as a series of elastic tubes of constant radii which changed stepwise distally from the aorta, a tube of slight taper was considered in the solution to avoid the difficulties presented by discontinuities in radii.

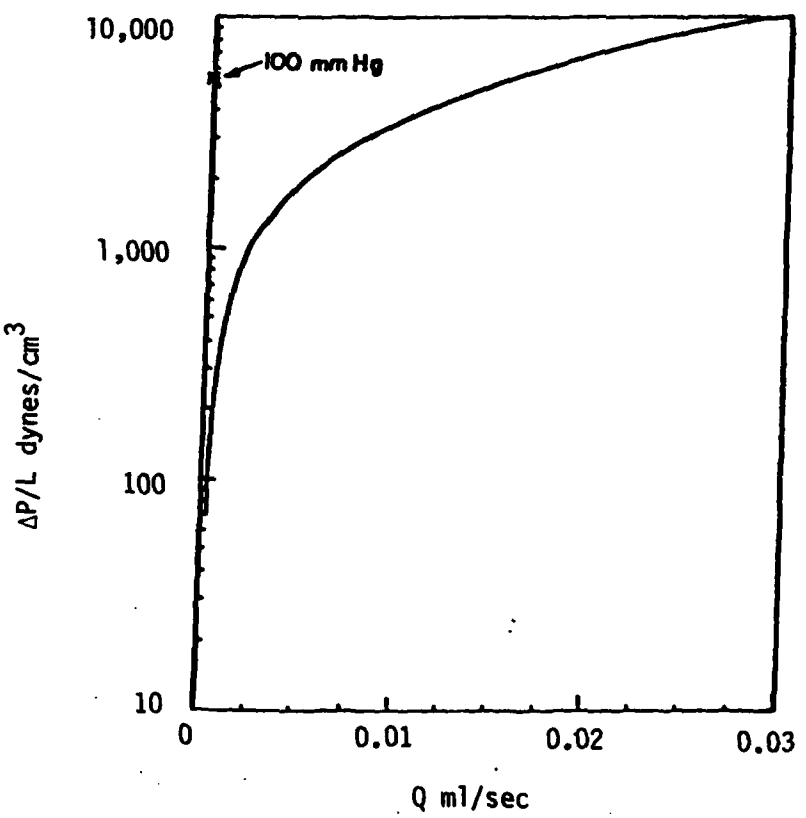

Fig. 6 Pressure - flow relationship for a narrow blood vessel (Eq.40)

Table I. Numerical Data on Arterial Segments

Name of Artery	Length $\Delta\ell$ (cm)	Internal radius r (cm)	Wall Thickness h (cm)	Volume $Q = \pi r^2 \Delta\ell$ (cm^3)
Aorta ascendens	2.0	1.47	0.164	13.571
Aorta ascendens	2.0	1.44	0.161	13.028
Arcus aorta	2.0	1.12	0.132	7.881
Arcus aorta	3.9	1.07	0.127	14.027
Aorta thoracalis	5.2	0.999	0.120	16.303
Aorta thoracalis	5.2	0.675	0.090	7.443
Aorta thoracalis	5.2	0.645	0.087	6.796
Aorta abdominalis	5.3	0.610	0.084	6.196
Aorta abdominalis	5.3	0.580	0.082	5.601
Aorta abdominalis	5.3	0.548	0.078	5.000
A.iliaca communis	5.8	0.368	0.063	2.467
A.iliaca externa	5.8	0.290	0.055	1.532
A.iliaca externa	2.5	0.290	0.055	0.660
A.profundus	6.3	0.255	0.052	1.287
A.profundus femoris	6.3	0.186	0.046	0.685
A.femoralis	6.1	0.270	0.053	1.397
A.femoralis	6.1	0.259	0.052	1.285
A.femoralis	6.1	0.249	0.051	1.188
A.femoralis	6.1	0.238	0.050	1.085
A.femoralis	7.1	0.225	0.049	1.129
A.poplitea	6.3	0.213	0.048	0.898
A.poplitea	6.3	0.202	0.047	0.807
A.poplitea	6.3	0.190	0.046	0.705
A.tibialis posterior	6.7	0.247	0.051	1.284
A.tibialis posterior	6.7	0.219	0.049	1.009
A.tibialis posterior	6.7	0.192	0.046	0.776
A.tibialis posterior	6.7	0.165	0.044	0.573
A.tibialis posterior	5.3	0.141	0.041	0.331
A.tibialis anterior	7.5	0.130	0.039	0.398
A.tibialis anterior	7.5	0.030	0.039	0.398
A.tibialis anterior	7.5	0.130	0.039	0.398
A.tibialis anterior	7.5	0.130	0.039	0.398
A.tibialis anterior	4.3	0.130	0.039	0.228
A.anonyma	3.4	0.620	0.086	4.106
A.subclavia	3.4	0.423	0.067	1.911
A.subclavia	6.8	0.403	0.066	3.969
A.axillaris	6.1	0.364	0.062	2.539
A.axillaris	5.6	0.314	0.057	1.734
A.brachialis	6.3	0.282	0.055	1.574
A.brachialis	6.3	0.266	0.053	1.400
A.brachialis	6.3	0.250	0.052	1.237
A.brachialis	4.6	0.236	0.050	0.804
A.ulnaris	6.7	0.215	0.049	0.972
A.ulnaris	6.7	0.203	0.047	0.867
A.ulnaris	6.7	0.192	0.046	0.776
A.ulnaris	3.7	0.183	0.045	0.389
A.radialis	7.1	0.174	0.044	0.675

Table I. (Cont.)

Name of Artery	Length $\Delta\ell$ (cm)	Internal radius r (cm)	Wall Thickness h (cm)	Volume $Q = \pi r^2 \Delta\ell$ (cm^3)
A.radialis	7.1	0.162	0.043	0.585
A.radialis	7.1	0.150	0.042	0.502
A.radialis	2.2	0.142	0.041	0.139
A.interossea volaris	7.9	0.091	0.028	0.205
A.coelica	1.0	0.390	0.064	0.478
A.gastrica sin.	7.1	0.180	0.045	0.723
A.lienalis	6.3	0.275	0.054	1.497
A.hepatica	6.6	0.220	0.049	1.003
A.renalis	3.2	0.260	0.052	0.679
A.mesenterica sup.	5.9	0.435	0.069	3.507
A.mesenterica inf.	5.0	0.160	0.043	0.402
A.carotis com. sin.	5.9	0.370	0.063	2.537
A.carotis com. sin.	5.9	0.370	0.063	2.537
A.carotis com. sin.	5.9	0.370	0.063	2.537
A.carotis com. sin.	3.1	0.370	0.063	1.333
A.car. int. sin.	5.9	0.177	0.045	0.581
A.car. int. sin.	5.9	0.129	0.039	0.308
A.cerebri anterior sin.	5.9	0.083	0.026	0.128
A.car. ext. sin.	5.9	0.177	0.045	0.581
A.car. ext. sin.	5.9	0.129	0.039	0.308
A.car. ext. sin.	5.9	0.083	0.026	0.128
A.car com. dextra	5.9	0.370	0.063	2.537
A.car. com. dextra	5.9	0.370	0.063	2.537
A.car. com. dextra	5.9	0.370	0.063	2.537
A.car. ext. dextra	5.9	0.177	0.045	0.580
A.car. ext. dextra	5.9	0.129	0.039	0.308
A.car. ext. dextra	5.9	0.083	0.026	0.127
A.car. int. dextra	5.9	0.177	0.045	0.581
A.car. int. dextra	5.9	0.129	0.039	0.308
A.cerebri anterior dex.	5.9	0.083	0.026	0.127
A.vertebralis	7.1	0.188	0.046	0.788
A.vertebralis	7.7	0.183	0.045	0.810

The following constants were used in the solution for arterial deformations:

R_0 = 1.47 cm

U = 11.9 cm/s

$\rho_w = \rho_0 = 1.05$ gr/cm^3

ν = 0.038 Stoke

A = 0.8

B = 11.35×10^4 dynes/cm^2

The flow chart of the solution technique for the comprehensive model is presented in Fig. 7. Assuming the pressure variation in the heart chamber as a cosine function varying between 80 and 120 mmHg, the entrance velocity into the aorta was calculated from the solution of Eq.(32). Coupling the linearized Navier-Stokes equations and the equations of motion for elastic tube deformation a solution was obtained for pressure and radius at various locations downstream from the aorta. The volume change can be calculated as a function of time from the computed radii.

Two acceleration profiles were used in the solution of the model proposed here. First, an impact type acceleration which was experimentally determined by Hanson[46] and shown in Fig. 8 was used and the aortic pressure was calculated. This pressure is shown in Fig. 9 in comparison with the pressure measured in the thoracic aorta of a beagle dog in response to the same acceleration profile. An exact quantitative comparison between the two pressure profiles is not possible because they were calculated for two different species having different physical dimensions and material properties. However, the qualitative comparison is quite satisfactory. Second, an acceleration profile measured during the flight of an F-14 aircraft was used to compute both radius and pressure in a segment of the aorta. The acceleration profile and the corresponding radius and pressure are shown in Figures 10, 11 and 12, respectively. The radius and pressure results of Figs. 11 and 12 were obtained for the 50-sec time domain indicated in Fig. 10. There are no pressure and radius data available for the F-14 acceleration profile for comparison. Such data is difficult to obtain noninvasively and there are understandably numerous restrictions against invasive measurements.

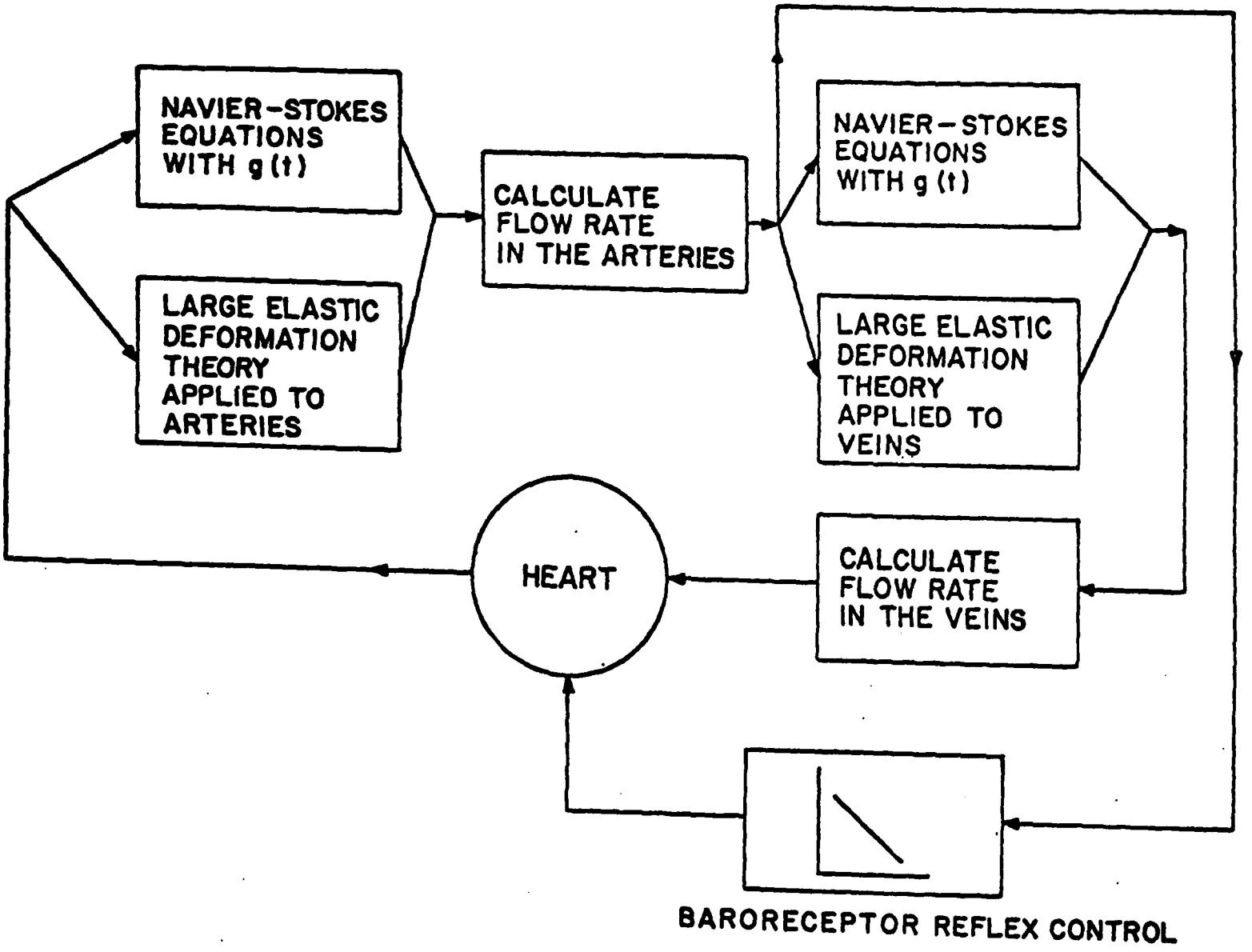

Fig. 7 Flow chart for solution technique

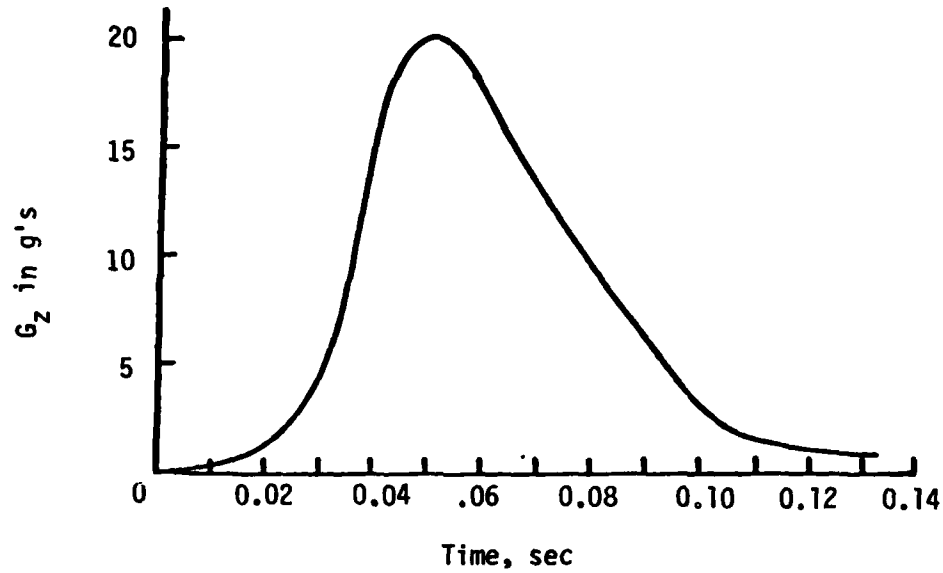

Fig. 8 Experimental deceleration profile measured by Hanson[46].

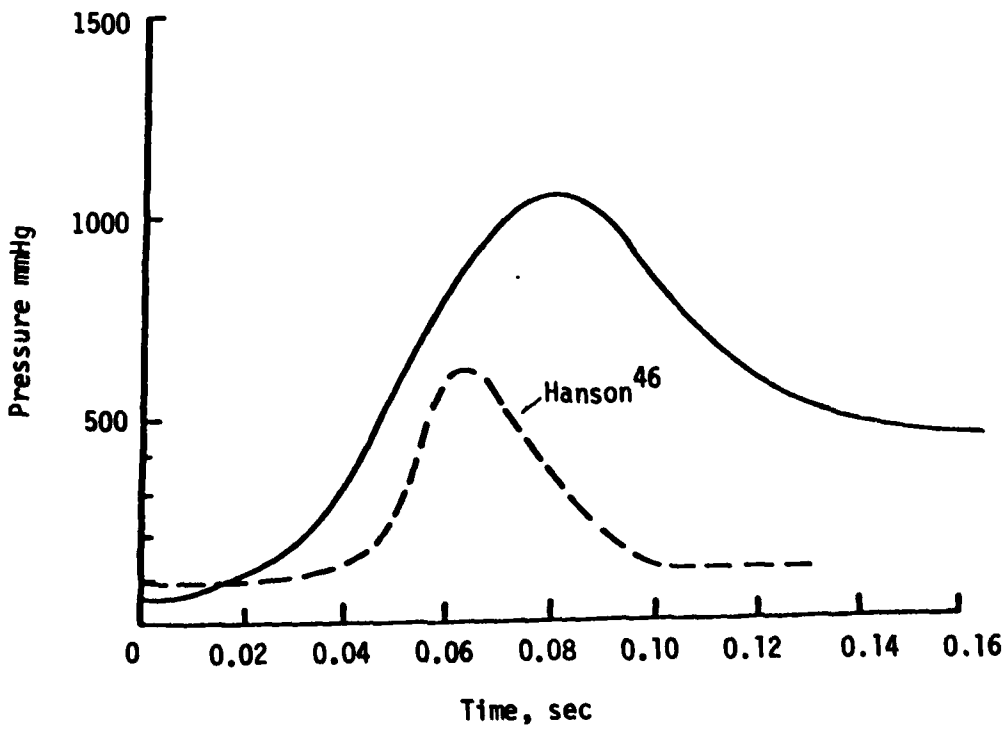

Fig. 9 Pressure in the aortic arch for Hanson's acceleration profile

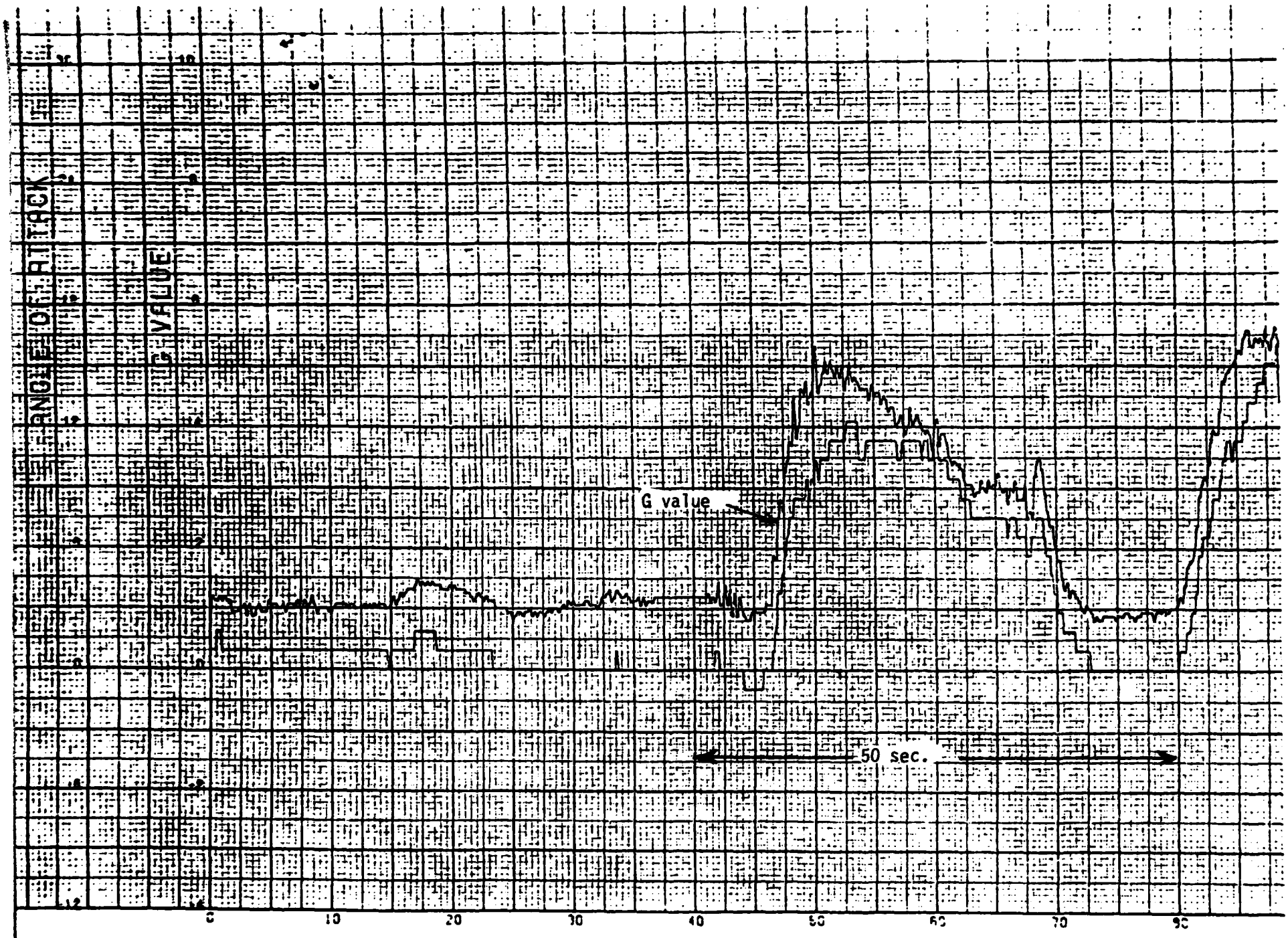

Fig. 10 G-profile for an F-14 flight

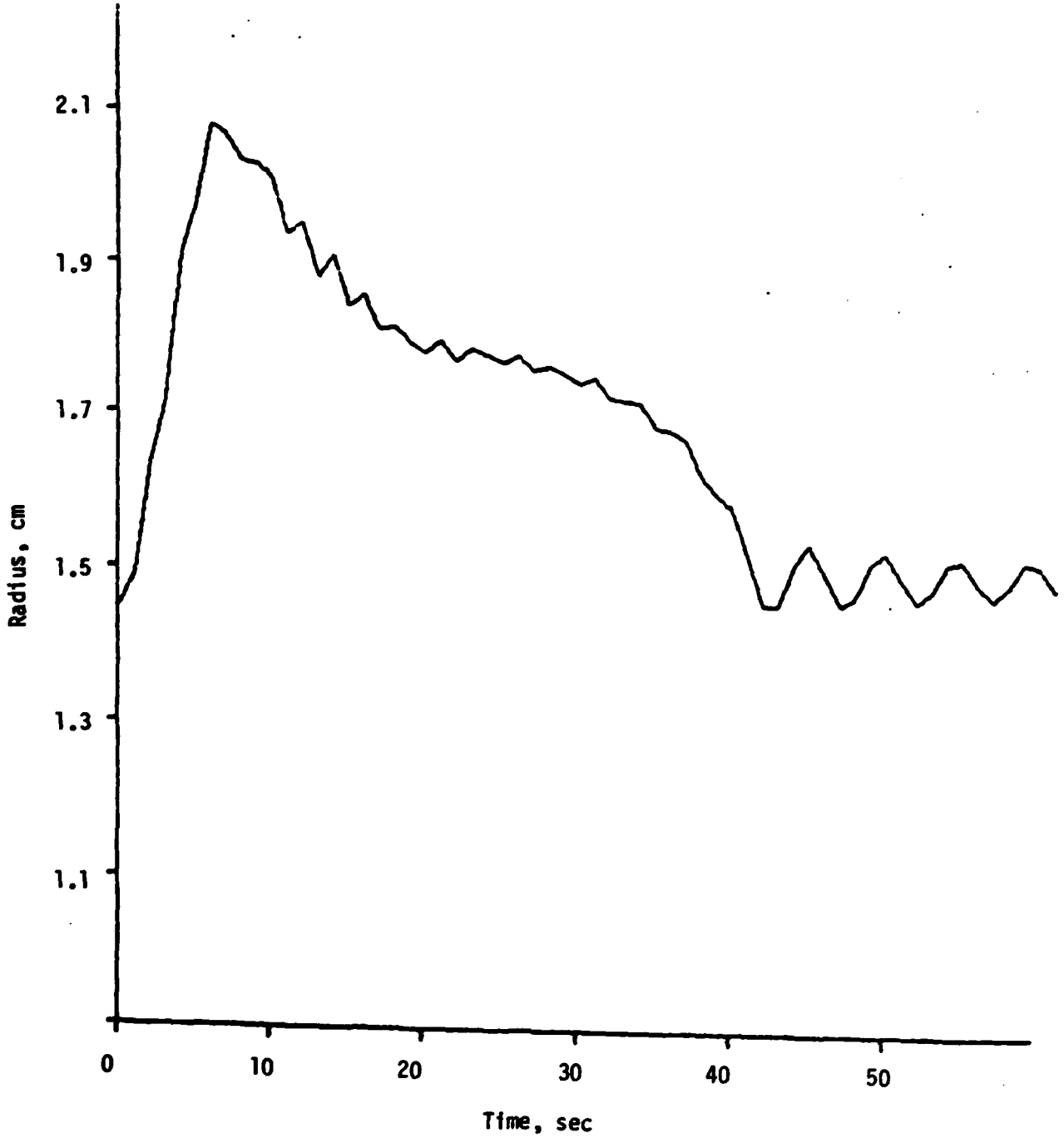

Fig. 11 Radius of aorta for the G-profile of F-14

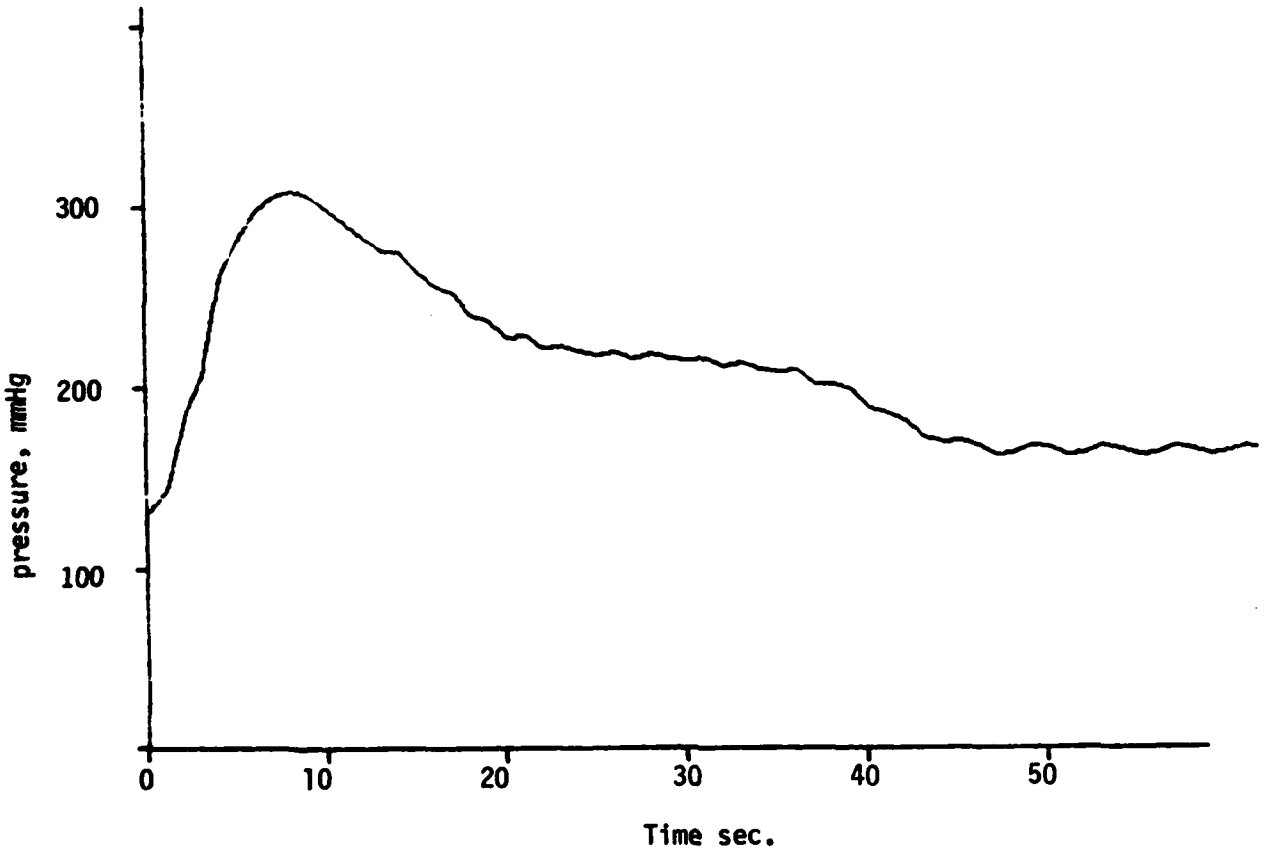

Fig. 12 Aortic pressure for G-profile of F-14

It should be apparent from Eqs.(25) and (32) that the blood flow response will depend upon the values assigned to the material constants A and B. To develop the total cardiovascular system model the values of A and B for all segments of arteries and veins in the body must be known. Such information is not available at the present time. Also, the numerical data on venous segments are not available for the complete venous system. However, in the present study it has been demonstrated that it is possible to construct an acceptable mathematical model of the cardiovascular system under acceleration stress by considering the mechanical parameters such as the physical dimensions, fluid properties and material properties of the blood vessels.

It is well known that finite-difference numerical procedures are time consuming and difficult to formulate for complex geometries of realistic shapes of the left ventricle and curves and branches in arteries and veins. Further study is recommended to formulate the model by finite element techniques by which complex geometries can be easily handled and computations can be more economically performed.

ACKNOWLEDGEMENT

The author wishes to acknowledge gratefully the encouragement received from Col. George W. Irving III, Program Manager, Life Sciences Directorate, Air Force Office of Scientific Research and Dr. Hans L. Oestreicher, former Chief, Mathematics and Analysis Branch, Air Force Aerospace Medical Research Laboratory, Wright-Patterson Air Force Base. Appreciation is also extended to Dr. James E. Whinnery and Dr. Kent K. Gillingham of the United States Air Force School of Aerospace Medicine, Brooks Air Force Base for providing access to the Acceleration Repository.

REFERENCES

1. Hiatt, E. P., Meechan, J. P., and Galambos, R., Reports on Human Acceleration, Publication 901, NAS-NRC, Washington, D.C.

2. Space Sciences Board, NAS-NRC, Physiology in the Space Environment Vol. 1 - Circulation, Publication 1485A, National Academy of Sciences, Washington, D.C., 1968.

3. Burton, R. R., Leverett, S. D., Jr., and Michaelson, E. D., "Man at High Sustained $+G_z$ Acceleration: A Review", Aerospace Medicine, 45, 1115-1136, 1974.

4. Womersley, J. R., "Mathematical Analysis of the Arterial Circulation in a State of Oscillatory Motion", Wright Air Development Center, Tech. Rept. WADC-TR-56-164, 1958.

5. Noordergraaf, A., "Hemodynamics", in Biological Engineering, Schwan, H., ed. McGraw-Hill, New York, 1969.

6. Taylor, M. D., "The Input Impedance of an Assembly of Randomly Branching Elastic Tubes", Biophysical J. 6, 25-51

7. Kenner, T., "Flow and Pressure in Arteries", in Biomechanics: It's Foundations and Objectives, Fung, Y. C. et al., eds., Prentice-Hall, Englewood Cliffs, New Jersey, 1972.

8. Attinger, E. O., Anne, T., Mikami, T., and Sugawara, H., "Modeling of Pressure Flow Relationships in Veins", in Hemorheology, Copley, A., ed., McGraw-Hill, New York, 1964.

9. Beneken, J. E. W., and DeWit, B., "A Physical Approach to Hemodynamic Aspects of the Human Cardiovascular System", in Physical Bases of Circulatory Transport: Regulation and Exchange, Reeve, E. B., and Guyton, A. C., eds., Saunders, Philadelphia, 1967.

10. Guyton, A. C., and Coleman, T. G., "Long Term Regulation of the Circulation: Interrelationship with Body Fluid Volumes", in Physical Bases of Circulatory Transport: Regulation and Exchange, Reeve, E. B., and Guyton, A. C., eds. Saunders, Philadelphia, 1967.

11. Pennock, B., and Attinger, E. D., "Optimization of the Oxygen Transport System". Biophysical J. 8, 879-96, 1968.

12. McLeod, J., "PHYSBE", Simulation, 10, 37-45, 1968.

13. Sagawa, K., "Overall Circulatory Regulation", in Annual Review of Physiology, 21, 295-330, Annual Reviews, Inc., Palo Alto, California, 1969.

14. Sagawa, K., "The Circulation and Its Control I: Mechanical Properties of the Cardiovascular System", in Engineering Principles in Physiology, 2, Brown, J. H. V., and Gann, D. S., eds., Academic Press, New York, 1973.

15. Camill, Jr., "Computer Modeling of Whole Body Sinusoidal Accelerations on the Cardiovascular System", Ph.D., dissertation, University of Kentucky, Lexington, Kentucky, 1971.

16. Boyers, D. G., Cuthbertson, J. G., and Luetscher, J. A., "Simulation of the Human Cardiovascular System" A Model with Normal Responses to Change of Posture, Blood Loss, Transfusion, and Autonomic Blockade", Simulation, 18, (6), 197-206, 1972.

17. Collins, R. E., Calvert, R. E., Hardy, H. H., and Jenkins, D. E., "Mathematical Simulation of the Cardiopulmonary System" AFOSR Progress Report, December 1978.

18. McDonald, D. A., Blood Flow in Arteries. E. Arnold (Publishers) Ltd., London, 1960.

19. Lambert, J. W., "On the Nonlinearities of Fluid Flow in Nonrigid Tubes", J. Franklin Inst., Vol. 26, pp. 83-102, 1958.

20. Skalak, R. and Stathis, T., "A Porous Tapered Elastic Tube Model of a Vascular Bed", in Biomechanics, Fung, Y. C., ed., ASME Symposium, New York, New York, 1966.

21. Kivity, Y. and Collins, R., "Nonlinear Wave Propagation in Viscoelastic Tubes: Application to Aortic Rupture", J. Biomechanics, Vol. 7, pp. 67-76, 1974.

22. Rudinger, G., "Shock Waves in Mathematical Model of the Aorta", J. Appl. Mech. ASME Vol. 37, pp. 34-37, 1970.

23. Bergel, D. H., "The Dynamic Elastic Properties of the Arterial Wall", J. Physiol. Vol. 156, pp. 458-469, 1961.

24. Fung, Y. C., "Elasticity of Soft Tissues in Simple Elongation", Am. J. Physiol. Vol. 213, pp 1532-1544, 1967.

25. Demiray, H., and Vito, R. P., "Large Deformation Analysis of Soft Biomaterials", Developments in Theoretical and Applied Mechanics, 8, Proc. 8th Southeast. Conf. on Theor. and Appl. Mech., pp. 515-522, 1976.

26. Prothero, J. and Burton, A. C., "The Physics of Blood Flow in Capillaries. I. The Nature of the Motion", Biophys. J. Vol. 1, pp. 565-579, 1961.

27. Whitmore, R. L., "A Theory of Blood Flow in Small Vessels", J. Appl. Physiol. Vol. 22, No. 4, pp. 767-771, 1967.

28. Gross, J. F. and Aroesty, J., "Mathematical Models of Capillary Flow: A Critical Review" Biorheology, pp. 225-264, Vol. 9, 1972.

29. Gross, J. F. and Intaglietta, M., "Effects of Morphology and Structural Properties on Microvascular Hemodynamics" Report No. P-5000, The Rand Corporation, Santa Monica, California, 1973.

30. Skalak, R., "Mechanics of the Microcirculation", in Biomechanics: It's Foundations and Objectives, Fung, Y. C. et.al. eds., Prentice Hall, Englewood Cliffs, New Jersey, 1972.

31. Fung, Y. C., "Microscopic Blood Vessels in the Mesentery", Biomechanics, Fung, Y. C., ed., ASME Symposium, New York, New York, 1966.

32. Burton, R. R., "Positive (+G_z) Acceleration Tolerances of the Miniature Swine: Application as a Human Analog", Aerosp. Med., Vol. 44, pp. 294-298, 1973.

33. Parkhurst, M. J., Leverett, S. D., Jr., and Shurbrooks, S. J., Jr., "Human Tolerance to High, Sustained +G_z Acceleration", Aerosp. Med., Vol. 43, pp. 708-712, 1972.

34. Leverett, S. D., Jr., Burton, R. R., Crossley, R. J., Michaelson, E. D., and Shurbrooks, S. J., Jr., "Physiologic Responses to High Sustained +G_z Acceleration", USAF School of Aerospace Medicine, Tech. Rep. No. 73-21, 1973.

35. Peterson, D. F., Bishop, V. S., and Erickson, H. H., "Cardiovascular Changes During and Following 1-min Exposure to +G_z Stress", Aviat. Space Environ. Med., Vol. 46, pp. 775-779, 1975.

36. Burton, R. R., and MacKenzie, W. F., "Heart Pathology Associated with Exposure to High Sustained G_z", Aviat. Space Environ. Med., Vol. 46, No. 10, pp. 1251-1253, 1975.

37. Green, A. E. and Zerna, W., Theoretical Elasticity, Oxford University Press, New York, London, 1968.

38. Klip, W., The Foundations of Medical Physics, University of Alabama Press, Birmingham, Alabama, 1969.

39. Kirchheim, H. R., "Systemic Arterial Baroreceptor Reflexes", Physiological Reviews, 56, (1), 100-176, 1976.

40. Taylor, M. D., "The Input Impedance of an Assembly of Randomly Branching Elastic Tubes", Biophys. J. Vol. 6, pp. 25-51, 1966.

41. Rouse, H. (ed.) Advanced Mechanics of Fluids, Wiley, New York, 1959.

42. Burton, A. C., Physiology and Biophysics of the Circulation, Year Book Medical Publishers, Chicago, 1965.

43. Benis, A. M., "Laminar Flow of Power-Law Fluids Through Narrow Three-Dimensional Channels of Varying Gap.",Chem. Engr. Sci., Vol. 22, pp. 805-822, 1967.

44. Merrill, E. W., Benis, A. M., Gilliland, E. R., Sherwood, T. K., and Salzman, E. W., "Pressure-Flow Relations of Human Blood in Hollow Fibres at Low Flow Rates", J. Appl. Physiol. Vol. 20, No. 5, pp. 954-967, 1965.

45. Westerhof, N., "Analog Studies of the Human Systemic Arterial Tree, Journal of Biomechanics, Vol. 2, pp. 121-143, 1969.

46. Hanson, P.G., "Pressure Dynamics in Thoracic Aorta During Linear Deceleration", Journal of Applied Physiology Vol. 28, pp. 34, 1970.


DAT
FILM